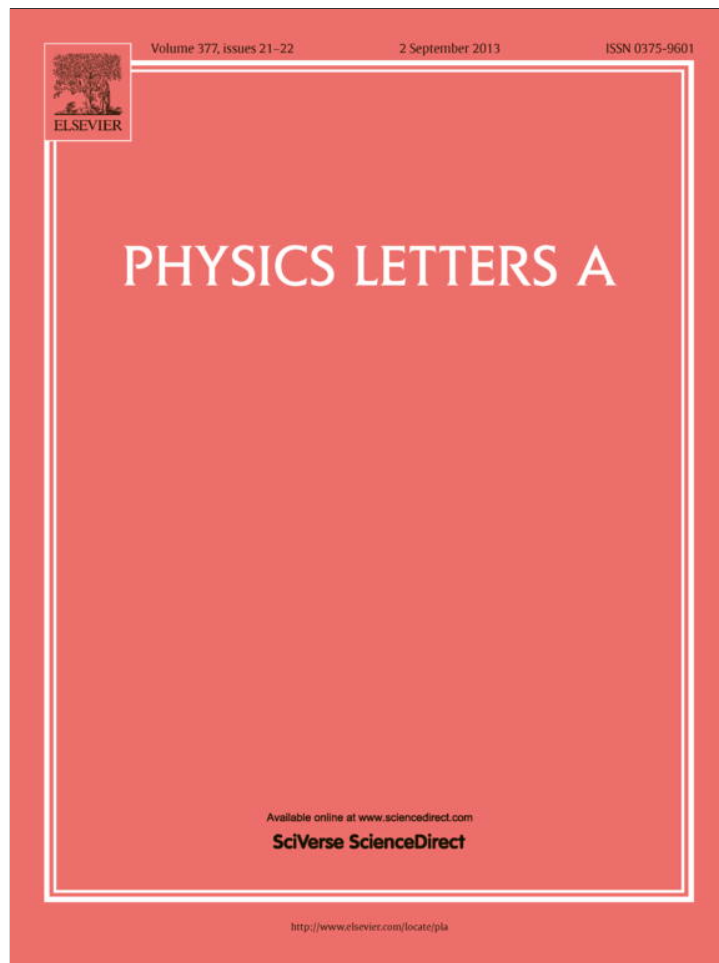


Provided for non-commercial research and education use.
Not for reproduction, distribution or commercial use.



This article appeared in a journal published by Elsevier. The attached copy is furnished to the author for internal non-commercial research and education use, including for instruction at the authors institution and sharing with colleagues.

Other uses, including reproduction and distribution, or selling or licensing copies, or posting to personal, institutional or third party websites are prohibited.

In most cases authors are permitted to post their version of the article (e.g. in Word or Tex form) to their personal website or institutional repository. Authors requiring further information regarding Elsevier's archiving and manuscript policies are encouraged to visit:

<http://www.elsevier.com/authorsrights>



Adjustable microwave permeability of nanorings: A micromagnetic investigation



Guozhi Chai*, Xinhua Wang, M.S. Si, Desheng Xue

Key Laboratory for Magnetism and Magnetic Materials of the Ministry of Education, Lanzhou University, 730000, Lanzhou, People's Republic of China

ARTICLE INFO

Article history:

Received 21 November 2012

Received in revised form 15 February 2013

Accepted 12 April 2013

Available online 15 April 2013

Communicated by A.R. Bishop

Keywords:

Microwave permeability

Nanoring

Micromagnetic simulations

ABSTRACT

Based on the three-dimensional micromagnetic simulations, we present a method to tailor the microwave permeabilities of magnonic metamaterials cells by a designed nanoring structure. The results show that the permeabilities and resonant frequency are depended on the wall's thickness of nanorings. The underlying mechanism is ascribed to the presence of strong demagnetization fields, which are associated to the ring's wall. In addition, the products of magnetic susceptibility and resonant frequency are larger than that predicted from Snoek's law in polycrystalline particles. These results are direct manifestations of the bi-anisotropy model.

© 2013 Elsevier B.V. All rights reserved.

Soft magnetic materials with suitable permeability at specific frequency are widely used in microwave devices, especially in metamaterials [1–4]. To obtain such magnetic materials is a quantity of interest both with respect to applied and fundamental investigation [5–9]. So it is valuable to find a material whose permeability can be adjusted in a wide band. According to some previous works, the determinative parameters to describe microwave permeability spectrum are static permeability μ_s , resonant frequency f_r and their product, i.e., Snoek's limit. In polycrystalline particles, $\mu_s - 1 = 2/3(4\pi M_s/H_k)$, and $f_r = \gamma H_k/(2\pi)$, where $4\pi M_s$ is the saturation magnetization, H_k is the effective anisotropic field and γ is the gyromagnetic factor. With the above relationships, it is easy to see that μ_s and f_r can be optimized in two ways. One is tailoring the magnitude of the anisotropic field H_k [10,11] or introducing an extra geometrical field upon scattering of spin waves [12]. Another way is adjusting the effective magnetization, e.g. changing content of the magnetic part in materials [13,14], optically induced magnetization [15].

However, based on Snoek's law [16], in polycrystalline particles, μ_s and f_r behave a competitive relation as $(\mu_s - 1)f_r = \frac{\gamma}{3\pi}4\pi M_s$. It is clear from this equation that, for certain materials, the enhancement of Snoek's limit is suppressed by M_s . Thus, it is still a huge challenge to obtain a magnetic material with high permeability as well as high resonant frequency simultaneously. An exceptional example, thin film with the uniform in-plane uniaxial anisotropy, is able to improve Snoek's limit by a factor $(4\pi M_s/H_k)^{1/2}$ [17,18]. In our previous work, Acher's limit can be enhanced in some spe-

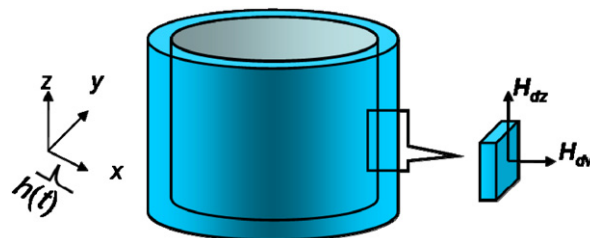


Fig. 1. (Color online.) The schematic picture of our model used in simulations. $h(t)$ is the exited field, and two demagnetization fields H_{dz} and H_{dw} are defined, respectively.

cial multilayer thin films, where an interface anisotropic field plays a key role [19]. These results suggested a clue for a higher Snoek's limit by introducing some typical anisotropic fields.

For thin films, the anisotropic field can be controlled in several ways [20–22]. But for nano-structured metamaterial cells, it is hard to adjust the anisotropic field in the normal ways. A new structure nanoring, as shown in Fig. 1, which holds a strong demagnetization field perpendicular to the wall, might be a promising candidate to adjust the permeability and enhance Snoek's limit only by changing the inner diameter. As to our knowledge, most of the previous works on nanorings are focus on ground states [23], hysteretic behaviors [24], phase diagrams [25], and spin dynamics [26–28]. Very recently, Wang et al. [29], have investigated the high frequency properties of nanorings, but their attention is limited at the resonant modes induced by the margin effect. Obviously, the investigation of microwave permeability and Snoek's limit in nanorings is missed, and the underlying mechanism is still unclear.

* Corresponding author.

E-mail addresses: chaigzh@lzu.edu.cn (G. Chai), xueds@lzu.edu.cn (D. Xue).

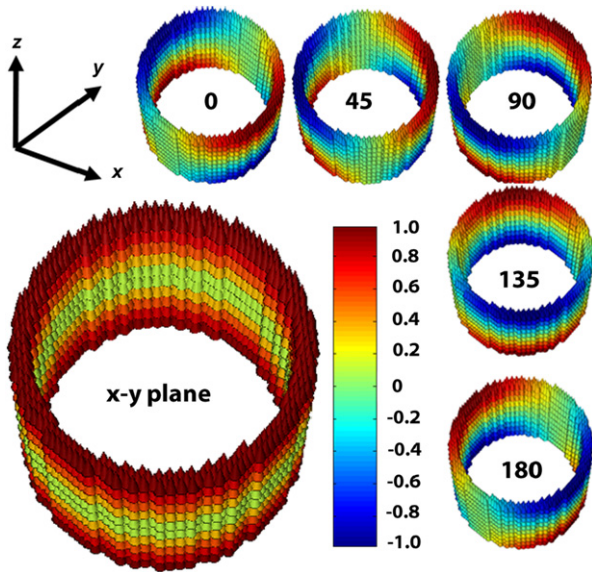


Fig. 2. (Color online.) The magnetization symmetry study of nanoring with $\sigma = 0.9$ at ground state. The numbers shown inside the rings are the investigated direction from x orientation with degree unit. The largest image shows the x - y plane magnetization dispersion of the nanoring.

Motivated based on the above discussions, in this Letter, we present a systematic three-dimensional micromagnetic simulation study of the high frequency susceptibility spectrum of nanorings as a function of geometric parameters (length L , inner diameter D_{in} , outer diameter D_{out} and ratio of the inner to the outer diameter σ) by using the object oriented micromagnetic framework package (OOMMF) [30]. The parameter σ allows us to adjust the demagnetization fields H_{dz} and H_{dw} , parallel and perpendicular to the nanoring's wall as shown in Fig. 1, which substantially determine the susceptibility and Snoek's limit. The $\mu_s - 1$ are adjusted from 20.3 to 0.7. Snoek's limits gradually decrease as σ changes from 0 to 0.9 because of the reducing effective magnetization, which is caused by the less magnetic ratio in the whole investigated cells.

The susceptibility spectrum can be obtained by the so-called field-pulse processes [31]. First, we obtained the stable state of the magnetizations via minimizing the total energy. The ground state can be found in Fig. 2. With magnetization symmetry study of nanoring with $\sigma = 0.9$, we can see that the magnetization dispersion shows the same behavior at different investigated direction. The results of x - y plane indicate that any direction in x - y plane is the symmetry directions. So, we select x direction as the investigated direction in the following parts for easier description. Then, the magnetization dynamics were then excited by a short, small field with the form $h(t) = 7.96 \times \exp(-7.675t)$ A/m, which is applied along the x axis as shown in Fig. 1. The time evolution of magnetization is thirdly characterized by solving the Landau-Lifshitz-Gilbert (LLG) equation. Finally, the frequency-dependent susceptibility spectrum is deduced from the Fourier transform of the time-dependent dynamic results. In metamaterial studies, the permeability normally was shown as effective permeability which is calculated by an averaging procedure of effective magnetization not only including the magnetic part, but also including the empty space of the investigated cells [14], so, the permeability results in this Letter were all recalibrated with this homogenization procedure.

The micromagnetic grid size is chosen as $0.5 \times 0.5 \times 2.0$ nm³, which is less than the exchange length l_{ex} [32]. The sampling mesh points are about $40 \times 40 \times 10$. This immediately imposes a big challenge in all the latter calculations, but guarantees the accuracy of our results. Material's parameters are those typical for

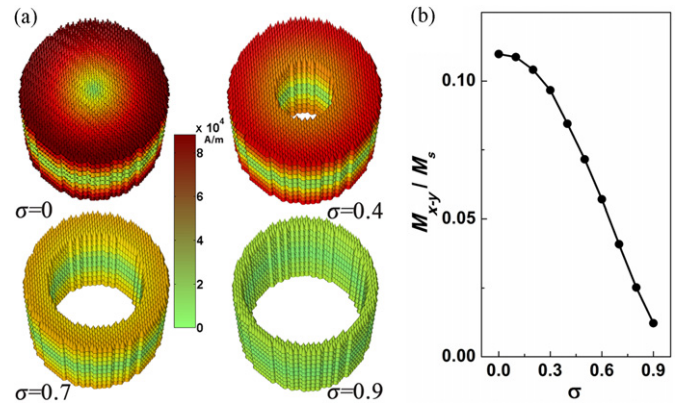


Fig. 3. (Color online.) (a) Magnetic moment patterns in the equilibrium state of Permalloy nanorings for different σ . The intensity map corresponds to the x - y plane component of magnetization normalized by the maximum value at $\sigma = 0$. (b) The maximum x - y components of normalized magnetization as a function of σ .

Permalloy: saturation magnetization $M_s = 8 \times 10^5$ A/m, exchange stiffness constant $A = 13 \times 10^{-12}$ J/m and null magnetocrystalline anisotropy. The damping parameters are used with 0.5 and 0.015 for the equilibrium and dynamical states, respectively. The exchange, demagnetization, and Zeeman energies are included during the simulated processes.

The model studied in this work is schematically shown in Fig. 1. Such model is designed to hold two types of anisotropic fields H_{dz} and H_{dw} simultaneously, which correspond to the one-dimensional nanowire and two-dimensional plane demagnetization fields. McMichael et al. [33] suggested a local magnetic resonance for the high frequency properties. Then the magnetic resonance should be discussed in local view as shown in Fig. 1. It is very crucial to improve Snoek's limit. The reason is that the permeability is only determined by the H_{dz} , while the resonant frequency depends on not only H_{dz} , but also the H_{dw} . This model is indeed a bi-anisotropy system proposed by our group [11], and thus Snoek's limit is predicted to be improved efficiently (see the discussions as follows). The corresponding demagnetization fields H_{dz} and H_{dw} are altered via changing the inner to the outer diameter σ in nanorings. As the x - y plane is isotropy, the x - y component of the magnetization was investigated to show the dispersion of the spins in x - y plane. Fig. 3(a) shows the calculated equilibrium magnetic moment patterns in Permalloy nanorings for four different σ . The dominant feature is that the equilibrium magnetization pattern is a nearly uniform magnetized state except for some small dispersed magnetic moments close to the ends of rings. Note that the color map is the magnetization of each cells compare with the magnetization of Permalloy 8×10^5 A/m. In particularly, the maximum magnetization at x - y component of magnetization as function of σ , which is normalized by saturation magnetization, is given in Fig. 3(b). As σ increases, the x - y component of magnetization first decreases slowly and then sharply. It implies the enhancement of H_{dz} and H_{dw} in these nanorings.

Fig. 4(a) and (b) shows the susceptibility spectrum of Permalloy nanorings with different σ changing from 0.1 to 0.9. Only one resonant peak is observed in the susceptibility spectrums. This indicates the uniform resonance occurs in these nanorings. The susceptibility and the resonant frequency as a function of σ are shown in Fig. 4(c) and (d), respectively. The results show that the resonant frequency increases from 1.3 GHz to 8.8 GHz while σ increasing from 0 to 0.9. In contrast, the static susceptibility shows an opposite trend decreasing from 20 to 0.7. The susceptibility $\mu_s - 1$ and the resonant frequency f_r indeed behave a competition relation, which is understandable from Snoek's law. The underlying microscopic mechanism can be attributed the enhancement of

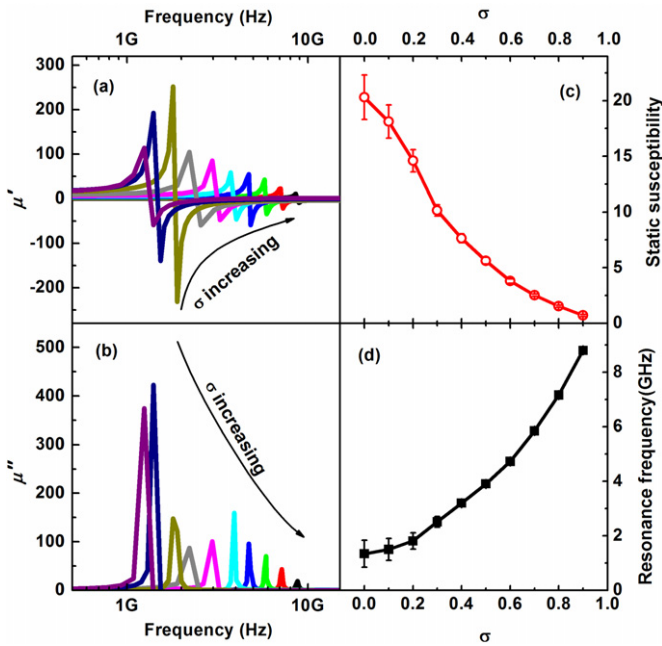


Fig. 4. (Color online.) The calculated magnetic spectrums for real (a) and imaginary part (b) of susceptibility, respectively. The static susceptibility (c) and resonant frequency (d) of Permalloy nanorings depend on σ . The error bars were from the simulation accuracy and Fourier transform.

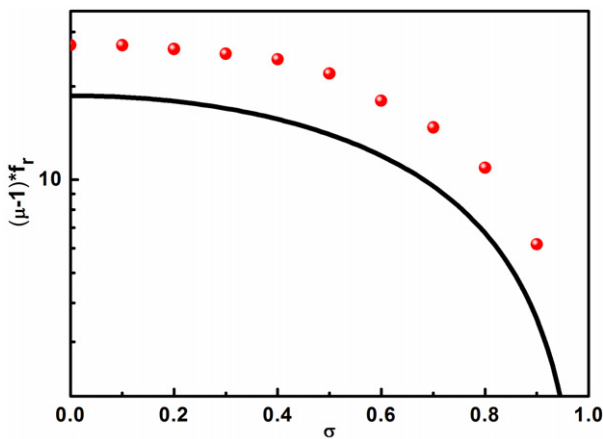


Fig. 5. (Color online.) Comparison of Snoek's limit of the nanorings and polycrystalline particles (solid black line). The red ball denotes the simulated results of nanorings with length 20 nm and σ changes from 0.1 to 0.9.

demagnetization field along z component H_{dz} [34]. The resonant frequency f_r is proportional to the effective field H_{dz} from the LLG equation; on the contrary, the susceptibility $\mu_s - 1$ varies inversely with H_{dz} . The reason is that the resonant frequency and susceptibility respectively behaves a different dependence on the anisotropic fields.

As Snoek's limit is proportional to M_s , so Snoek's limit should be decreased with the σ increasing due to the reduced effective magnetization in susceptibility calculation. Snoek's limit of polycrystalline particles is shown in Fig. 5 with dark solid curve. Snoek's limit of nanoring is improved obviously compared to that in the polycrystalline particles, which can be found in Fig. 5 with red solid ball. The physical mechanism is that the demagnetization field H_{dw} increases with the σ increasing and the magnetization are all lie in the wall at z direction with the large demagnetization. According to the discussion therein before, Snoek's limit can be improved. As σ increases, Snoek's limit of nanoring first slightly

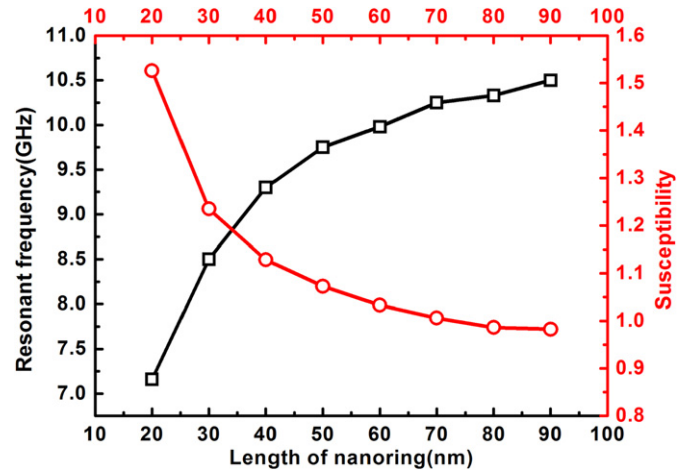


Fig. 6. (Color online.) The static susceptibility (red circle) and resonant frequency (dark square) of Permalloy nanorings depend on length of nanorings with $\sigma = 0.8$.

decreases which nearly parallel to the solid curve, and then sharp decreases after $\sigma > 0.4$. This behavior is due to the relative volume reducing of the magnetic nanoring.

In order to adjust the resonant frequency of nanorings in wider range, we study the length effect on the resonant frequency of nanoring. The high frequency properties of nanorings with different length from 20 to 90 nm at $\sigma = 0.8$ can be found in Fig. 6. It explicitly shows that the resonant frequency can be adjusted from 7.2 to 10.5 GHz. Such variation comes from the enhancement of the axial demagnetization field. Furthermore, based on Kittel equation, the resonant frequency can be adjusted in a wider range with an applied extra static field.

V.S. Tkachenko et al. found that in curved nanowires, the curvature leads to a "geometrical" effective magnetic field term that is proportional to the square of the ratio of the exchange length to the radius of curvature of the waveguide, which are very interesting [12]. This induced effective field can reduce the whole effective magnetic field in the curved nanowires. Then the resonant frequency lower down due to the reduced effective magnetic field at waveguide direction. However, in the nanoring structures studied in this Letter, the uniform magnetization directions are all at z direction as shown in Fig. 2, which are different with the nanowires. This "geometrical" effective magnetic field term in nanoring is too small to induce a considerable effect on the high frequency property of single nanoring cell with uniform resonance. Further study will focus on this phenomenon in a multiple nanoring structures if any.

In summary, the susceptibility and the resonant frequency of nanorings are studied in this work. The simulated results show that the resonant frequency can be adjusted from 1.3 GHz to 8.8 GHz and the susceptibility behaves from 20 to 0.7 by changing the demagnetization field H_{dw} perpendicular to the wall of nanoring. In addition, the resonant frequency can reach as much as 10.5 GHz by extending the nanoring's length to 90 nm. All Snoek's limits of nanorings predicted in our work are higher than that in polycrystalline particles. Snoek's limits of nanorings are controlled cooperatively by the uniform magnetized state and the effective demagnetization field H_{dw} . Our work provided a new metamaterial with an adjustable microwave permeability, which substantially exceed Snoek's limit.

Acknowledgements

This work is supported by the National Basic Research Program of China (No. 2012CB933101) and National Natural Science Foun-

dition of China (NSFC) (Nos. 51107055, 11034004, and 50925103). We are grateful to Shanghai Supercomputer Center for using its computational resources.

References

- [1] V.V. Kruglyak, P.S. Keatley, A. Neudert, R.J. Hicken, J.R. Childress, J.A. Katine, *Phys. Rev. Lett.* **104** (2010) 027201.
- [2] V.V. Kruglyak, S.O. Demokritov, D. Grundler, *J. Phys. D: Appl. Phys.* **43** (2010) 264001.
- [3] S. Neusser, H.G. Bauer, G. Duerr, R. Huber, S. Mamica, G. Woltersdorf, M. Krawczyk, C.H. Back, D. Grundler, *Phys. Rev. B* **84** (2011) 184411.
- [4] S. Neusser, G. Duerr, S. Tacchi, M. Madami, M.L. Sokolovskyy, G. Gubbiotti, M. Krawczyk, D. Grundler, *Phys. Rev. B* **84** (2011) 094454.
- [5] S.X. Wang, N.X. Sun, M. Yamaguchi, S. Yabukami, *Nature* **407** (2000) 150.
- [6] Y.W. Zhao, X.K. Zhang, J.Q. Xiao, *Adv. Mater.* **17** (2005) 915.
- [7] S.H. Yu, M. Yoshimura, *Adv. Funct. Mater.* **12** (2002) 9.
- [8] G.Z. Chai, D.W. Guo, X.L. Fan, D.S. Xue, *Sci. China Phys. Mech.* **54** (2011) 1200.
- [9] G.Z. Chai, D.S. Xue, X.L. Fan, X.L. Li, D.W. Guo, *Appl. Phys. Lett.* **93** (2008) 152516.
- [10] C. Kittel, *Phys. Rev.* **73** (1948) 155.
- [11] D.S. Xue, F.S. Li, X.L. Fan, F.S. Wen, *Chin. Phys. Lett.* **25** (2008) 4120.
- [12] V.S. Tkachenko, A.N. Kuchko, M. Dvornik, V.V. Kruglyak, *Appl. Phys. Lett.* **101** (2012) 152402.
- [13] M. Mruczkiewicz, M. Krawczyk, R.V. Mikhaylovskiy, V.V. Kruglyak, *Phys. Rev. B* **86** (2012) 024425.
- [14] O. Dmytriiev, M. Dvornik, R.V. Mikhaylovskiy, M. Franchin, H. Fangohr, L. Giovannini, F. Montoncello, D.V. Berkov, E.K. Semenova, N.L. Gorn, A. Prabhakar, V.V. Kruglyak, *Phys. Rev. B* **86** (2012) 104405.
- [15] R.V. Mikhaylovskiy, E. Hendry, V.V. Kruglyak, *Phys. Rev. B* **86** (2012) 100405(R).
- [16] J.L. Snoek, *Physica* **14** (1948) 207.
- [17] O. Acher, A.L. Adenot, *Phys. Rev. B* **62** (2000) 11324.
- [18] O. Acher, S. Dubourg, *Phys. Rev. B* **77** (2008) 104440.
- [19] G.Z. Chai, Y.C. Yang, J.Y. Zhu, M. Lin, W.B. Sui, D.W. Guo, X.L. Li, D.S. Xue, *Appl. Phys. Lett.* **96** (2010) 012505.
- [20] O. Acher, J.L. Vermeulen, P.M. Jacquart, J.M. Fontaine, P. Baclet, J. Magn. Mater. **136** (1994) 269.
- [21] Y. Fu, Z. Yang, T. Miyao, M. Matsumoto, X.X. Liu, A. Morisako, *Mater. Sci. Eng. B* **133** (2006) 61.
- [22] X.L. Fan, D.S. Xue, M. Lin, Z.M. Zhang, D.W. Guo, C.J. Jiang, J.Q. Wei, *Appl. Phys. Lett.* **92** (2008) 222505.
- [23] S.P. Li, D. Peyrade, M. Natali, A. Lebib, Y. Chen, U. Ebels, L.D. Buda, K. Ounadjela, *Phys. Rev. Lett.* **86** (2001) 1102.
- [24] J. Rothman, M. Kläui, L. Lopez-Diaz, C.A.F. Vaz, A. Bleloch, J.A.C. Bland, Z. Cui, R. Speaks, *Phys. Rev. Lett.* **86** (2001) 1098.
- [25] W. Zhang, R. Singh, N. Bray-Ali, S. Haas, *Phys. Rev. B* **77** (2008) 144428.
- [26] G. Gubbiotti, M. Madami, S. Tacchi, G. Carlotti, H. Tanigawa, T. Ono, L. Giovannini, F. Montoncello, F. Nizzoli, *Phys. Rev. Lett.* **97** (2006) 247203.
- [27] J. Podbielski, F. Giesen, D. Grundler, *Phys. Rev. Lett.* **96** (2006) 167207.
- [28] Z.K. Wang, H.S. Lim, H.Y. Liu, S.C. Ng, M.H. Kuok, L.L. Tay, D.J. Lockwood, M.G. Cottam, K.L. Hobbs, P.R. Larson, J.C. Keay, G.D. Lian, M.B. Johnson, *Phys. Rev. Lett.* **94** (2005) 137208.
- [29] J.B. Wang, B. Zhang, Q.F. Liu, Y. Ren, R.L. Liu, *J. Appl. Phys.* **105** (2009) 083908.
- [30] M.J. Donahue, D.G. Porter, OOMMF User's Guide, Version 1.2a3, <http://math.nist.gov/oommf>, 2002.
- [31] O. Gérardin, H. Le Gall, M.J. Donahue, N. Vukadinovic, *J. Appl. Phys.* **89** (2001) 7012.
- [32] R.D. McMichael, B.B. Maranville, *Phys. Rev. B* **74** (2006) 024424.
- [33] R.D. McMichael, D.J. Twisselmann, A. Kunz, *Phys. Rev. Lett.* **90** (2003) 227601.
- [34] M. Beleggia, J.W. Lau, M.A. Schofield, Y. Zhu, S. Tandon, M. De Graef, *J. Magn. Mater.* **301** (2006) 131.